Available online at www.sciencedirect.com
ScienceDirect
International Journal of Mass Spectrometry 263 (2007) 267–275
International Journal of Mass Spectrometry
www.elsevier.com/locate/ijms

Quantum chemical calculations on the structure and stability of $Mg^{2+}XH_3OH$ complexes in the gas phase (X = C, Si, and Ge)

Ahmed M. El-Nahas *, Safinaz H. El-Demerdash, El-Sayed E. El-Shereefy

Chemistry Department, Faculty of Science, El-Menoufia University, Shebin El-Kom, Egypt

Received 2 February 2007; received in revised form 4 March 2007; accepted 5 March 2007
Available online 12 March 2007

Abstract

The structure and stability of $Mg^{2+}XH_3OH$ complexes in gas phase (X = C, Si and Ge) have been studied using the B3LYP/6-31 + G(d) and CBS-QB3 levels of theory. Several dissociation pathways for $Mg^{2+}XH_3OH$ complexes have been investigated. The complexes are thermodynamically stable with respect to the loss of H^+, OH^+, XH_3, XH_4, and XH_4^+ but thermodynamically unstable toward the loss of XH_3^+, XH_3OH^+, and XH_3O^+ ions. The presence of sizable kinetic energy barriers (25–81 kcal/mol) for unimolecular dissociation hinders the exothermic processes. This indicates that $Mg^{2+}XH_3OH$ complexes can form metastable species and is likely observed under appropriate experimental conditions. On the other hand, endothermic channels are unlikely occurred under mild experimental conditions. Binding energies in the investigated complexes parallel charge transfer from ligands to the Mg^{2+} ion. Comparison between B3LYP and CBS-QB3 results is also presented.

Keywords: Monosolvated Mg dication; Stability; Methanol; Silanol; CBS-QB3; B3LYP

1. Introduction

Although gas-phase metal–ligand complexes have been studied for several decades, most work was limited to singly charged species because solvated multiply charged metal ions were not accessible until the 1990s [1,2]. Thermodynamically stable ligated metal dication $M^{2+}L$ can exist if the ionization energy (IE) of M^+ is lower than the first IE of the ligand L. In such situation the electrostatic interaction between M^{2+} and L gives rise to a bound $M^{2+}L$. Even if the IE of M^+ is slightly exceeded IE of L, the $M^{2+}L$ may be thermodynamically stable, provided that the binding energy of $M^{2+}L$ compensates for the difference in IEs. Upon further increase of IE of M^+, the $M^{2+}L$ becomes metastable with respect to the dissociation into M^+ and L^+. This kind of dissociation is referred to as charge separation reaction or "Coulomb explosion" [3]. Despite the thermodynamically favored separation reaction, the $M^{2+}L$ complex can exist as a metastable species providing that such dissociation step is hindered by an energy barrier. This is called kinetically stable ligated metal dications.

The existence of multiply charged metal ions with a limited number of neutral ligands in the gas phase has attracted attention over the past decade [1,2,4–32]. The experimental difficulty in generating dictation of metals with a single solvent ligand tends to increase with increasing difference between the second IE of metals and the first IE of a solvent. Two parameters have been introduced to characterize the stability of multicharged systems against dissociation [1,2,4–6,11–26]. These are defined as minimum (n_{min}) and critical (n_{crit}) number of ligands. The minimum number of ligands represents those ligands required to stabilize the action center whereas the critical number stands for number of ligands above which the loss of neutral ligand become more favorable than the dissociative electron and proton transfer. Higher values of n_{min} and n_{crit} indicate lower complex stability and propensity for reduction.

Magnesium, one of the most common elements, plays an important role in biological systems [33–36]. Magnesium prefers binding to phosphate, carboxylate, hydroxyl and ether oxygens because it is a hard metal [33]. Experimental studies on magnesium dication with alcohols have been performed for methanol and propanol using pick-up technique [6,26]. The experiments showed that at least two methanol and three propanol molecules, respectively, are needed to stabilize the dication centre. The minimum number of ligands needed to

* Corresponding author.
E-mail address: amelnahas@hotmail.com (A.M. El-Nahas).

1387-3806/$ – see front matter © 2007 Elsevier B.V. All rights reserved.
doi:10.1016/j.ijms.2007.03.002

stabilize Mg^{2+} center was 2, 3, and 3 for CH_3OH, C_2H_5OH, and n-C_3H_7OH, respectively [26]. Four ROH molecules are needed to form stable $Mn^{2+}(ROH)_n$ complex in the gas phase ($R = CH_3$, CH_3CH_2–, $CH_3CH_2CH_2$–, and $(CH_3)_2CH$–) [5]. On the other hand, no stable $Pb^{2+}(ROH)_n$ complexes could be found for $R = CH_3$ and CH_3CH_2– [4]. Nevertheless, $Pb^{2+}(ROH)_n$ was observed for $R = CH_3CH_2CH_2$– and $CH_3CH_2CH_2CH_2$– with $n \geq 3$ [4].

Using the same experimental technique, Wright et al. have reported that three molecules from methanol, 2-propanol, or acetone are able to form stable dication complexes with copper dication [13]. Copper has an IE2 of 20.3 eV compared to 15.0 eV for magnesium [37] and is expected to have lower tendency to form stable complexes. Three acetone molecules are needed to stabilize the Mg^{2+} ion, while no complexes could be detected for DMSO with Mg^{2+} using pick-up experimental technique [26]. However, Shvartsburg et al. observed Mg^{2+}DMSO in the gas phase using electrospray ionization (ESI) technique [16].

Quantum chemical calculations have also contributed to the progress of finite solvated multicharged ion chemistry [38–55]. Existence of monoligated metal dications complexes with water, ammonia, acetone, DMSO have been confirmed by theoretical calculations for a variety of alkaline-earth and first-row transition metals [38–55]. The computational predictions have been confirmed by a number of experimental works [14,16,31,32]. Acetone and DMSO ligands have lower ionization energies (9.7 and 9.1 eV, respectively) compared to methanol (10.8 eV) [56] and even though form stable monoligated complexes with magnesium dications [38]. Therefore, methanol is expected to form stable complex when reacts with Mg^{2+}. However, there is still a lack of theoretical investigations on alcohols with magnesium dication in the gas phase, especially regarding to the issue of existence or non-existence of alcohol monoligated Mg^{2+} ion in the gas phase. In this respect we believe that quantum chemical calculations would be a very helpful tool for this topic. Therefore, an important feature of the present study is to predict the possibility of detecting methanol and silanol monoligated magnesium dication in the gas phase. Germanol (heavier analogue of methanol and silanol) has also been included for comparison.

2. Computational methods

All electronic structure calculations were performed using the Gaussian98W suite of programs [57]. Geometry optimizations for XH_3OH molecules, $Mg^{2+}XH_3OH$ complexes (X = C, Si, and Ge), and their reaction products have been performed using Density Functional Theory (DFT) at the B3LYP [58–60] level with 6-31 + G(d) basis sets. For each stationary point, we carried out vibrational frequency calculation to characterize their nature as minima or transition states and to correct energies for zero-point energy and thermal contribution. The transition states for some unimolecular dissociation channels have been located using several techniques, including the synchronous transit-guided quasi-Newton (QST2 and QST3) and the eigenvalue-following (EF) optimization procedures as implemented in the Gaussian programs. The nature of the transition states was confirmed by the presence of one negative eigenvalue in the Hessian matrix. The vibrational modes were examined by using the ChemCraft program [61]. Partial charge distributions were calculated using the natural population analysis (NPA) method [62]. The stability of the electronic wave functions was confirmed with the *stable* option of Gaussian98W.

With the exception of germanium containing systems, the energies of all species were calculated using the complete basis set method (CBS-QB3) [63,64]. The CBS-QB3 procedures combine the results of several electronic structure calculations and empirical terms to predict molecular energies to around 1 kcal mol^{-1} accuracy [65]. Accuracy in structure and energies requires convergence in basis set size and in the degree of correlation; the dilemma is that both expansion of the basis set and increasing the degree of correlation adds significantly to the cost of the calculation. The philosophy of implementation is that instead of using additive corrections to account for the limitations of the basis set, as in the G*n* methods, results for different levels of theory are extrapolated to the CBS limit [66]. The five-step CBS-QB3 series of calculations starts with a geometry optimization at the B3LYP/6-311G(d,p) level followed by a frequency calculation at the same level. The Frequencies are scaled by a factor of 0.99. The next three computations are single-point calculations (SPCs) at the CCSD(T), MP4SDQ, and MP2 levels. The CBS extrapolation then computes the final energies.

The biradical character of the transition states that correspond to the loss of XH_3OH^+, XH_3^+, XH_3O^+ has been taken into account for one of them, namely the transition state for the loss of CH_3OH^+, from $Mg^{2+}CH_3OH$, using the UBL3/6-311G(d,p) method with the guess = mix option. This choice facilitates a spin-unrestricted description of systems with a multiplicity of one. The results obtained from this reassessment are identical with the previous ones. In view of this finding, the remaining transition states of biradical character were not subjected to the guess = mix analysis.

3. Results and discussion

3.1. Structures

3.1.1. XH_3OH and XH_3OH^+

The optimized structures of XH_3OH molecules, $Mg^{2+}XH_3OH$ complexes, and transition states for three dissociation channels are given in Fig. 1. The corresponding geometrical parameters are collected in Tables 1 and 2. Structural parameters of different dissociation reaction fragments are presented in supporting information. NPA atomic charges from the B3LYP/6-311G(d,p) density for various species are listed in Tables 3 and 4. Geometry optimization at CBS-QB3 uses the B3LYP/6-311G(d,p) level and will be used for discussion unless noted otherwise.

Our computed geometrical parameters for methanol are in good agreement with the values calculated [67] at the MP2/6-311 + G(2d,p) and QCISD/6-31G(d) levels of theory as well as with experiment [68]. The only difference between theory and experiment was found for the HOC bond angles of 2–3°. In

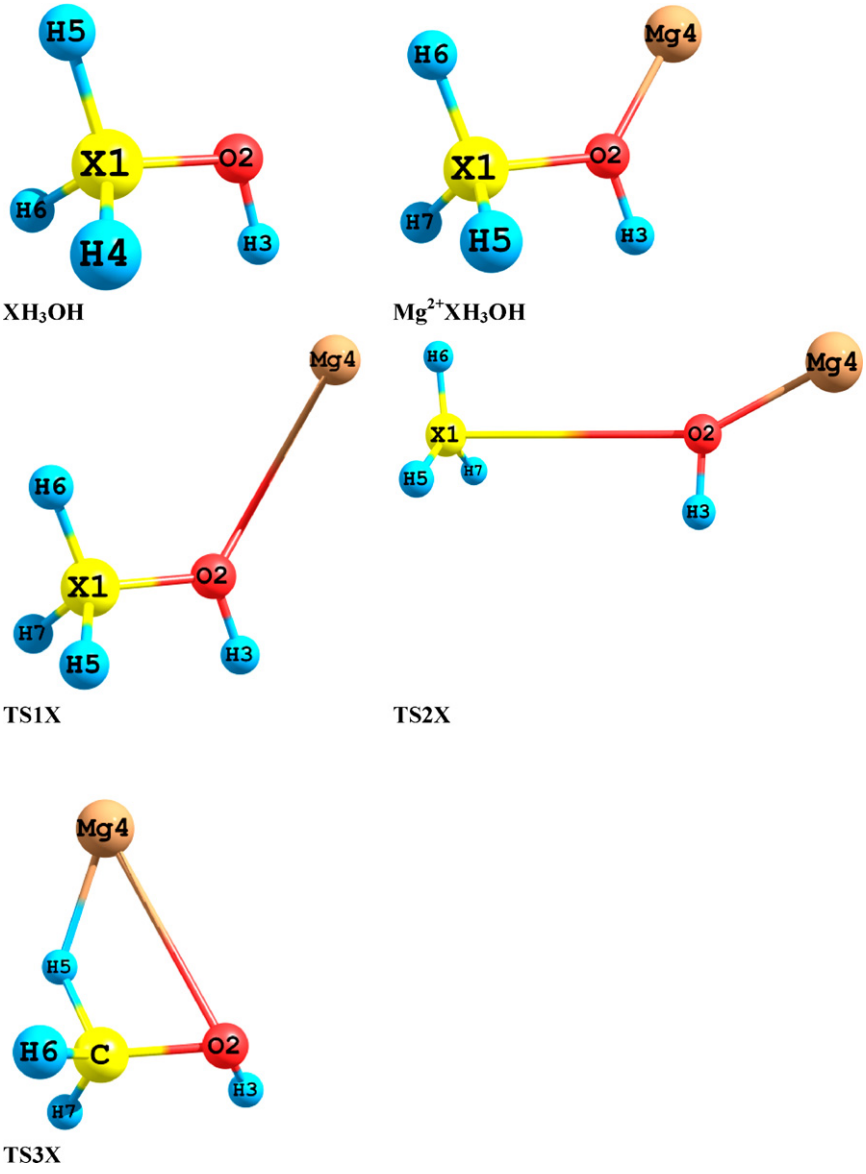

Fig. 1. Optimized structures of XH_3OH, $Mg^{2+}XH_3OH$ and transition states for dissociation (X = C, Si, and Ge).

Table 1
Geometrical parameters for CH_3OH, CH_3OH^+, $Mg^{2+}CH_3OH$, and transition states at B3LYP/6-311G(d,p)[a,b]

Parameters	CH_3OH	CH_3OH^+	$Mg^{2+}CH_3OH$	TS1	TS2	TS3
R(1-2)	1.421	1.359	1.542	1.407	3.609	1.341
R(1-5)	1.099	1.087	1.087	1.085	1.092	1.316
R(1-6)	1.099	1.129	1.087	1.114	1.092	1.091
R(1-7)	1.091	1.128	1.087	1.108	1.092	1.095
R(2-3)	0.961	0.985	0.974	0.974	0.964	0.973
R(2-4)			1.892	4.206	1.799	3.006
A(2-1-5)	112.5	116.7	106.4	109.1	87.2	110.6
A(2-1-6)	112.5	106.4	106.3	109.4	96.7	113.4
A(2-1-7)	106.9	106.5	106.3	111.8	87.2	118.9
A(1-2-3)	107.8	114.3	107.1	109.0	87.0	113.6
A(1-2-4)			130.8	132.5	152.1	68.2
A(5-1-6)	108.6	115.2	111.9	110.5	119.9	100.2
A(5-1-7)	108	115.2	111.9	112.4	120.2	95.9
A(6-1-7)	108	94.1	113.5	103.6	119.9	114.6
A(3-2-4)			122.1	112.6	121.0	127.1

[a] Atom numbering is given in Fig. 1.
[b] Bond lengths are given in Angstrom and angles in degrees.

Table 2
Geometrical parameters for SiH_3OH, SiH_3OH^+, $Mg^{2+}SiH_3OH$, and transition states at B3LYP/6-311G(d,p)[a,b]

Parameters	SiH_3OH	SiH_3OH^+	$Mg^{2+}SiH_3OH$	TS1Si	TS2Si	TS3Si
R(1-2)	1.653	1.640	1.770	1.682	3.714	1.605
R(1-5)	1.484	1.471	1.573	1.463	1.467	1.810
R(1-6)	1.475	1.627	1.463	1.510	1.467	1.464
R(1-7)	1.484	1.469	1.463	1.508	1.467	1.467
R(2-3)	0.959	0.974	0.974	0.97	0.965	0.968
R(2-4)			1.918	4.238	1.8	3.366
A(2-1-5)	111.9	109.8	86.3	106.3	83.5	93.9
A(2-1-6)	105.7	86.8	111.1	106	92.7	115.5
A(2-1-7)	111.9	116.8	111	109.2	93.8	119.5
A(1-2-3)	119	127.6	123.2	115.7	88.0	129.5
A(1-2-4)			98.0	136.1	152.4	75.8
A(5-1-6)	109.8	102.6	109.2	117.2	120	93.7
A(5-1-7)	107.8	124.7	109.1	114.7	119.9	98.2
A(6-1-7)	109.8	107.9	123.7	103	120.1	122.4
A(3-2-4)			138.8	106	119.7	140

[a] Atom numbering is given in Fig. 1.
[b] Bond lengths are given in Angstrom and angles in degrees.

Table 3
NPA atomic charges for CH_3OH, CH_3OH^+, $Mg^{2+}CH_3OH$, and transition states at B3LYP/6-311G(d,p)[a]

Atom/fragment	CH_3OH	CH_3OH^+	$Mg^{2+}CH^3OH$	TS1	TS2C	TS3C
Mg			1.929	1.483	1.806	1.826
C1	−0.185	−0.213	−0.146	−0.193	0.336	−0.003
O2	−0.715	−0.242	−1.005	−0.517	−1.267	−0.646
H3	0.441	0.534	0.559	0.499	0.498	0.533
H5	0.145	0.238	0.200	0.210	0.209	−0.204
H6	0.145	0.342	0.231	0.270	0.209	0.234
H7	0.169	0.342	0.231	0.248	0.209	0.260
CH_3OH	1E-05	1	0.071	0.517		
MgH						1.622
CH_2OH						0.378
CH_3					0.963	

[a] Atom numbering is given in Fig. 1.

CH_3OH^+, the ionization leads to slightly decrease in C–O bond length by 0.062 Å and OH increases by 0.024 Å. Two C–H bonds are also elongated by 0.037 and 0.030 Å. Both OCH and HCH bond angles increase of by 4.2° and 6.6°, respectively.

For silanol, our calculated Si–O and OH bond lengths (1.653 and 0.959 Å) are in good agreement with the values obtained at the CCSD(T)/cc-pVDZ level (1.651 and 0.959 Å) [69]. On the other hand, the SiOH angle is smaller at the latter level (116.9°) compared to the B3LYP/6-311G(d,p) value of 119.0°. Up ionizing the SiH_3OH molecule, the Si–O shortens by 0.013 Å, while one of the out-of-plane Si–H is elongated by 0.152 Å with the corresponding HSiO angle decreases by 18.9°. On the other hand, the HOSi and HSiH angles are enlarged by 8.6° and 16.9°, respectively.

Table 4
NPA atomic charges for SiH_3OH, SiH_3OH^+, $Mg^{2+}SiH_3OH$, and transition states at B3LYP/6-311G(d,p)[a]

Atom/fragment	SiH_3OH	SiH_3OH^+	$Mg^{2+}SiH_3OH$	TS1Si	TS2Si	TS3Si
Mg			1.893	1.460	1.800	1.816
Si1	1.204	1.235	1.266	1.174	1.354	1.516
O_2	−1.050	−0.785	−1.233	−0.931	−1.282	−1.098
H_3	0.487	0.553	0.580	0.516	0.497	0.567
H_5	−0.221	−0.060	−0.368	−0.142	−0.125	−0.584
H_6	−0.200	0.149	−0.069	−0.031	−0.122	−0.110
H_7	−0.221	−0.093	−0.069	−0.047	−0.123	−0.108
SiH_3OH	0.0	1.0	0.107	0.540		
MgH						1.232
SiH_2OH						
SiH_3					0.985	0.768

[a] Atom numbering is given in Fig. 1.

At the B3LYP/6-31 + G(d) level and as given in Table 5S, on going from neutral to monopositive GeH_3OH, the Ge–O bond length is elongated by 0.037 Å and one of the out-of-plane Ge–H bonds is elongated by 0.074 Å with the corresponding OGeH angle being contracted by 26.5°. The HOGe angle is enlarged by 7.1°.

3.1.2. Interaction of Mg dication with XH_3OH molecules

Reaction of Mg^{2+} ion with a single XH_3OH molecules gives $Mg^{2+}XH_3OH$ dication complexes. Once the dicationic complex is formed, it can undergo a variety of dissociation channels which can be summarized as follows:

(a) Dissociation back to reactants:

$$Mg^{2+}XH_3OH \rightarrow Mg^{2+} + XH_3OH$$

(b) Dissociation to monopositive fragments (charge transfer):
- (i) $Mg^{2+}XH_3OH \rightarrow Mg^{+} + XH_3OH^{+}$
- (ii) $Mg^{2+}XH_3OH \rightarrow MgOH^{+} + XH_3^{+}$
- (iii) $Mg^{2+}XH_3OH \rightarrow MgH^{+} + XH_3O^{+}$
- (iv) $Mg^{2+}XH_3OH \rightarrow MgOXH_3^{+} + H^{+}$
- (v) $Mg^{2+}XH_3OH \rightarrow MgXH_3^{+} + OH^{+}$
- (vi) $Mg^{2+}XH_3OH \rightarrow MgO^{+} + XH_4^{+}$

(c) Dissociation to neutral and charged dications:
- (i) $Mg^{2+}XH_3OH \rightarrow MgO^{2+} + XH_4$
- (ii) $Mg^{2+}XH_3OH \rightarrow MgOH^{2+} + XH_3$

Dissociation to monopositive fragments represents charge separation (electron transfer), whereas processes (a) and (c) show a loss of neutral species. Transition states for the exothermic channels and slightly endothermic ones (i, ii, and iii) were located.

For XH_3OH molecules, their coordination with Mg^{2+} increases the X–O bond lengths by 0.183 and 0.117 Å for X = C and Si, respectively. Similarly, the O-H bond distances are increased by 0.011 and 0.015 Å for X = C and Si. However, the in-plane X–H bond increases by 0.012 and 0.089 Å for X = C and Si. The XOH angle decreases by 0.7° for X = C while increases by 4.2° for X = Si. The $OXH_{in\text{-}plane}$ angle shows no change for X = C, but significantly decreases for X = Si; by 25.6°. This is because of the attraction between negatively charge hydrogen atom (−0.368e for X = Si) and positively charged Mg atom (+1.893e for X = Si), while H (+0.200e) of CH and Mg (+1.929e) atoms bear positive charges.

For the $Mg^{2+}CH_3OH$ complex, the NPA negative charge on oxygen atom increases by 0.290e, while hydrogens gain more positive charges. On the other hand, the negative charge over carbon atom decreases by 0.039e. This indicates that the CH_3OH molecule is polarized by Mg^{2+} dication. The charge distribution over CH_3OH in the complex of +0.071e reveals a small but definite transfer of negative charge from CH_3OH to Mg^{2+} dication which results in a slight reduction of the dipositive charge on Mg atom to +1.929e (see Table 3). The same behavior was also found for $Mg^{2+}SiH_3OH$ system (Table 4).

In the transition states a total charge of +2e is imposed on the whole system. Therefore, we could differentiate between the loss of charged or neutral species from charge distribution over fragments. The transition states located for the dissociation of $Mg^{2+}CH_3OH$ dication to $Mg^{+} + CH_3OH^{+}$, $MgOH^{+} + CH_3^{+}$, and $MgH^{+} + CH_3O^{+}$ are designated as TS1C, TS2C, and TS3C, respectively. Frequency analysis shows that the negative frequencies in the transition states correspond to the relevant reaction vector namely Mg–O, O–C, and (Mg–O, Mg–H, and C–H) bonds, respectively. The Mg–O bond in TS1C is significantly elongated in the transition state compared to the $Mg^{2+}CH_3OH$ dication complex (4.206 Å versus 1.892 Å). Moreover, the C–O bond length in TS1C optimized to a value intermediate between that in the neutral and monopositive CH_3OH molecules. This indicates that a significant amount of positive charge has been transferred from Mg^{2+} to CH_3OH in the transition state (+0.517 and +1.483e over CH_3OH and Mg, respectively) (Table 3). This should be compared with +0.071 and +1.929e over CH_3OH and Mg in the $Mg^{2+}CH_3OH$. In other word, the transition state structure is somehow between reactant and product. In the TS2C, the C–O bond is significantly elongated (3.609 Å versus 1.542 Å) and the charge over CH_3 is +0.963e indicating a product-like structure according to Hammond postulate [70]. The transition state for the loss of MgH^{+} (TS3C) shows an elongation of C–H and Mg–O bonds by 0.229 and 1.114 Å, respectively, while forming Mg–H bond of 1.798 Å compared to bond length in the free MgH^{+} molecule of 1.658 Å. The NPA charge over the MgH and CH_2OH fragments in the TS3C are +1.622 and +0.379e, respectively, which indicates a reactant-like structure. The same geometrical and electronic changes have been found on going from $Mg^{2+}XH_3OH$ (X = Si, Ge) to different transition states as shown in Tables 2 and 4, Tables 3S–6S.

At B3LYP/6-31 + G(d) and CBS-QB3, all products optimized to the desired structures expect XH_3O^{+} ions which gradually transformed to XH_2OH^{+} isomers. From the study of the CH_3O^{+} species, it is firmly established that the most stable form is that of hydroxymethyl cation, CH_2OH^{+} [71]. Similarly, SiH_3O^{+} and GeH_3O^{+} optimize to SiH_2OH^{+} and GeH_2OH^{+} ions, respectively. The structures of the XH_3OMg^{+} fragments indicate bending at the oxygen atom which decreases from C to Ge, 144.0°, 164.0°, and 178.1°, respectively, at the B3LYP/6-31 + G(d). Moreover, the Mg–O bond lengths decrease from X = C to Ge, 1.773, 1.751, and 1.737 Å, respectively.

3.2. Energetics

Relative energies with respect to $Mg^{2+}XH_3OH$ complex are depicted in Figs. 2–4. All energies were corrected for ZPEs. Total energies of all species are collected in supporting information. Binding energies (BEs) were calculated by subtracting total energies of Mg^{2+} and XH_3OH from those of $Mg^{2+}XH_3OH$.

The energy difference between the transition state and the corresponding $Mg^{2+}XH_3OH$ complex defines the energy barrier of the respective dissociation process. For all processes, the dissociation energy is defined as the difference between the zero-point corrected total energies of the dissociation products and the magnesium dication complex.

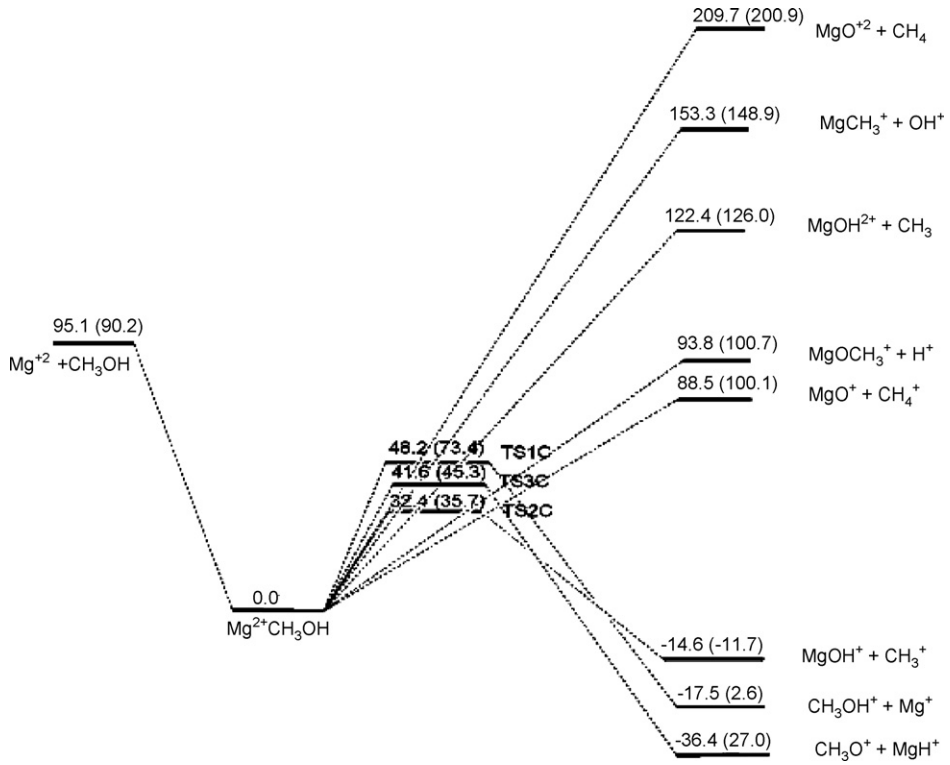

Fig. 2. Energy profile (zero-point corrected relative energies (kcal/mol)) for the formation and dissociation of $Mg^{2+}CH_3OH$ at B2LYP/6-31 + G(d), CBS-QBS-QB3 results are given in parentheses.

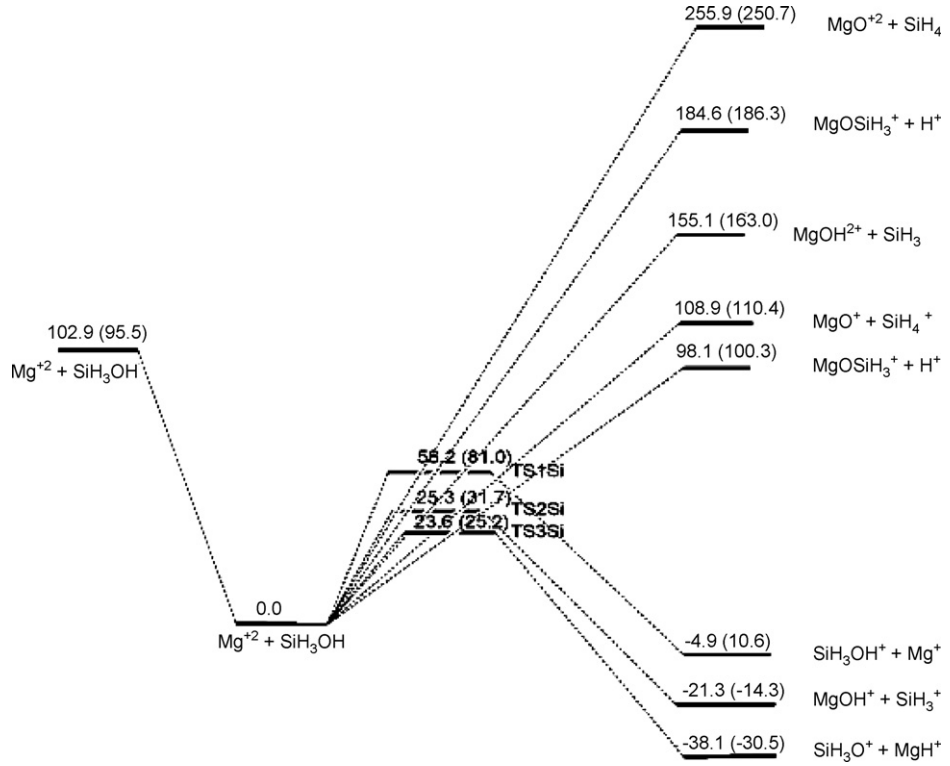

Fig. 3. Energy profile (zero-point corrected relative energies (kcal/mol)) for the formation and dissociation of $Mg^{2+}SiH_3OH$ at B3LYP/6-31 + G(d), CBS-QB3 results are given in parentheses.

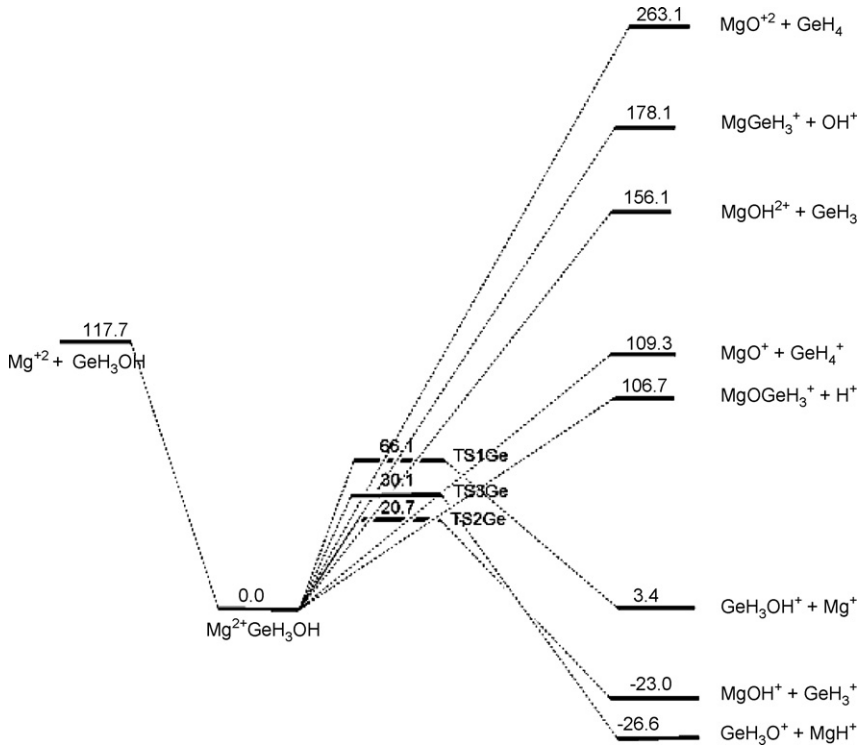

Fig. 4. Energy profile (zero-point corrected relative energies (kcal/mol)) for the formation and dissociation of $Mg^{2+}GeH_3OH$ at B3LYP/6-31 + G(d).

The BEs of investigated Mg dication with XH_3OH molecules do not follow the electrostatic bonding which is proportional to $Z\mu/r^2$ and indicates that the smaller the interatomic distance between ligand and Mg^{2+} ion the larger the BE. In addition, dipole moments of CH_3OH and SiH_3OH of 1.714 (exp.: 1.700 [37]) and 1.422 Debye, respectively, at the B3LYP/6-311G(d,p) level also do not parallel the binding energy order of the two ligands of 92.2 and 95.5 kcal/mol. However, the binding energies parallel the amount of charge transfer from the ligands to metal center (see Tables 3 and 4).

Since CBS-QB3 calculations include correlation energies at CCSD(T)/6-31 + G(d) based of B3LYP/6-311G(d,p) geometry we can compare binding energies of the species investigated in this work with other systems calculated at CCSD(T). The binding energies of $Mg^{2+}XH_3OH$ complexes of 90.2 (X = C) and 95.5 (X = Si) kcal/mol are large than that of $Mg^{2+}H_2O$ system of 75.9 kcal/mol at the CCSD(T)/6-311 + G(d,p)//B3LYP/6-311 + G(d,p) level [42] and $Mg^{2+}CH_2O$ of 86.1 kcal/mol at the CCSD(T)/6-311 + G(d,p)//B3LYP/6-31 + G(d) level [38]. This indicates that the interaction between the Mg^{2+} with XH_3OH ligands is stronger than that in H_2O and CH_2O molecules.

The results given in Figs. 2–4 indicate that reactions (a), (b-iv), (b-v), (b-vi), and (c) are all energy demanding processes (highly endothermic) and unlikely occur except when higher temperature is provided to the reaction system. On the other hand, channels i, ii, and iii are exothermic where the dissociation products are thermodynamically stable with respect to the dication complexes. This indicates that unimolecular dissociation paths i, ii, and iii can occur spontaneously unless sufficient kinetic energy barriers exist to hinder such transformation. The IE2 of Mg was calculated as 14.7 eV, which compares well with the experimental value of 15.0 eV [37]. The IE2 of Mg is larger than the IE1 of XH_3OH of 10.9 and 11.0 eV for X = C and Si, respectively, at the CBS-QB3 level. The value of 10.9 eV for CH_3OH is in good agreement with the experimental value of 10.8 eV [56]. Because of this difference in the ionization energies and in the absence of stabilizing effect, it is expected that charge transfer should occur spontaneously. Transition states for pathways i, ii, and iii do exist with sizable energy barriers that grant kinetic stability to the $Mg^{2+}XH_3OH$ dication complexes and, therefore, they should be observed with appropriate experimental conditions.

As shown in Figs. 2 and 3, the $Mg^{2+}XH_3OH$ dications are thermodynamically stable species with respect to loss of H^+, XH_3, OH^+, XH_4, and XH_4^+, while unstable toward the loss of XH_3^+, XH_3OH^+, and XH_3O^+ fragments. $Mg^{2+}CH_3OH$ is thermodynamically unstable with respect to dissociation to $Mg^+ + CH_3OH^+$, $MgOH^+ + CH_3^+$, and $MgH^+ + CH_3O^+$. $Mg^{2+}SiH_3OH$ is slightly thermodynamically unstable with respect to dissociation to $Mg^+ + SiH_3OH^+$, and more unstable toward dissociation to $MgOH^+ + SiH_3^+$ and $MgH^+ + SiH_3O^+$. Based only on this thermodynamic behavior, one cannot expect observation of $Mg^{2+}CH_3OH$ and $Mg^{2+}SiH_3OH$ experimentally as they will dissociate spontaneously to monopositive fragments mentioned earlier. Nevertheless, the presence of sizable energy barriers hinders such molecular dissociation and the $Mg^{2+}CH_3OH$ and $Mg^{2+}SiH_3OH$ complexes can be observed experimentally.

At the B3LYP/6-31 + G(d) level, $Mg^{2+}GeH_3OH$ is kinetically and thermodynamically stable toward dissociation to $Mg^+ + GeH_3OH^+$, but thermodynamically unstable toward dissociation to $MgOH^+ + GeH_3^+$ and $MgH^+ + GeH_3O^+$ (Fig. 4).

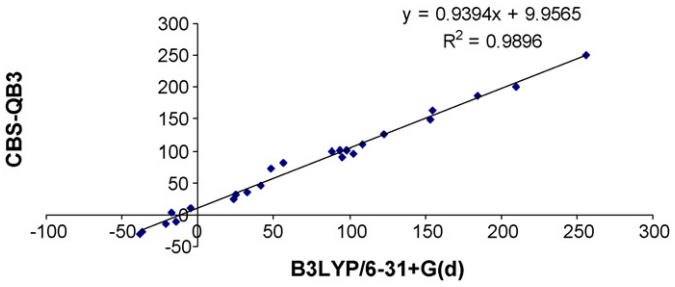

Fig. 5. Zero-point corrected binding and dissociation energies (kcal/mol) for $[MgCH_3OH]^{2+}$ and $[MgSiH_3OH]^{2+}$ systems.

However, these latter channels are hindered by kinetic energy barriers and the $Mg^{2+}GeH_3OH$ complex also should exist and, therefore, can be observed.

An inspection of Figs. 2 and 3 reveals that at the B3LYP/6-31 + G(d) level, the reaction energies for the loss of CH_3^+, CH_3OH^+, and CH_3O^+ are −14.6, −17.5, and −36.4 kcal/mol. On the other hand, these values at the CBS-QB3 level are −11.7, 2.6, and −27.0 kcal/mol, respectively. For $Mg^{2+}SiH_3OH$ dissociation, both B3LYP and CBS-QB3 predict the same order for the reaction energies. However, the big difference between B3LYP and CBS-QB3 results was noticed for the reaction energies related to the loss XH_3OH^+ of 20 and 15 kcal/mol for X = C and Si, respectively. This difference of 20 kcal/mol (0.9 eV) between B3LYP and CBS-QB3 for X = C may be attributed to the difference between the two methods in estimating the IE for Mg^+, 15.5 and 14.7 eV, respectively, compared to the experimental value of 15.0 eV [37]. The differences between the barrier heights for the loss of $XH_3OH^+ + Mg^+$ is 25 and 22 kcal/mol for X = C and Si, respectively.

Experimental work on Mg^{2+} with methanol clusters observed $Mg^{2+}(CH_3OH)_n$ with $n \geq 2$ [6,26]. Among the dissociation products of methanol ligated magnesium dication complexes, Mg^+OCH_3, $MgOH^+$, and MgH^+ fragment were recorded [6]. This findings agree with our computational results based the energy profile given in Fig. 2.

The DFT at the B3LYP level overestimates charge transfer (CT) contribution to binding energies (BEs) as reported previously [38–42]. CT contribution to BEs is non-negligible in the dication complexes under investigation as shown from NPA charges on magnesium and ligands in the dication complexes (Tables 3 and 4, Tables 2S, 4S, and 6S). Compared to CCSD(T), B3LYP underestimate barrier heights by 2–23 kcal/mol [38–42], which means that B3LYP energies cannot be used for kinetic studies where the exponential part in the rate equation is very sensitive to change in the value of the energy barrier.

Accuracy of B3LYP in calculating binding and dissociation energies of the $Mg^{2+}XH_3OH$ dication complexes depend on the presence or absence of charge transfer between metal ion and ligand. In cases where the charge transfer is negligible, B3LYP results are more accurate and vice versa.

Plot of different energies calculated at B3LYP against the corresponding values at CBS-QB3 is displayed in Fig. 5. The plot shows an impressive linear correlation. This good linear relation can be used to estimate accurate reaction energies and barrier heights for the germanium containing systems. However, in most cases B3LYP overestimates exothermicity of the reactions and underestimates the barrier heights compared to CBS-QB3 values.

Based on the high-level calculations used in this work, we could safely predict the possibility of detecting methanol monoligated magnesium dication complex and its heavier analogues in the gas phase using appropriate experimental conditions. Previous experimental studies using pick-up technique reported that at least two methanol molecules are needed to stabilize the magnesium dication center [6,26]. However, the pick-up method failed to observe water monoligated copper dication in the gas phase [12], while ESI and CS experimental methods detected such complex [14,31,32]. These two latter experimental procedures support our earlier theoretical work in this respect [39–41]. In addition, pick-up method [26] also failed to find a stable complex between Mg^{2+} ion and DMSO although ESI was able to do this job [16]. Failure to detect a species experimentally is not an evidence for its absence. Unfortunately, so far there are no ESI and CS investigations for the interaction of Mg^{2+} with methanol. For further understanding of the interaction of methanol with magnesium dication, theoretical calculations should be conducted on methanol di- and triligated Mg^{2+} ion to study different dissociation channels because intramolecular proton transfer was observed experimentally [6]. It is also worthwhile to compare the results with aproptic solvents where there is no labile proton. These will be the subject of future work.

4. Conclusion

In this paper we have studied theoretically the structure and stability of $Mg^{2+}XH_3OH$ complexes (X = C, Si and Ge) in gas phase and their possible dissociation channels to give evidence for detecting complexes of Mg^{2+} dication with a single XH_3OH molecule. The calculations have been done at the B3LYP/6-31 + G(d) and CBS-QB3 levels of theory.

The results obtained can be summarized as follows:

The interaction of the Mg^{2+} ions with the XH_3OH molecules forms $Mg^{2+}XH_3OH$ complexes. Binding energies in the complexes parallel charge transfer from ligands to the Mg^{2+} ion. Once the complexes are formed they can undergo a variety of dissociation channels.

Based on the thermodynamic criteria for reactions, the $Mg^{2+}XH_3OH$ should not be formed due to the existence of three exothermic channels, which means spontaneous dissociation of the complexes upon their formation. However, the presence of sizable energy barriers hinders such dissociation channels and result in kinetically stable monosolvated magnesium dication complexes in the gas phase.

Plot of binding and dissociation energies from B3LYP and CBS-QB3 calculations gives impressive correlation which can be used for estimating accurate reactions energies and barrier heights for ligated metal dication complexes when CBS-QB3 calculations are prohibitive for computer resources or other reasons as the case of germanium containing system reported here.

B3LYP method by its own seems to be inappropriate for calculation of accurate reaction energies and barrier height for the

formation and dissociation of ligated metal dications but can be used to study the relative importance of different pathways

The experimental work with the pick-up technique indicated that at least two methanol molecules are needed to stabilize the Mg^{2+} ion in the gas phase. As found previously for monosolvated water dication complex, the conflict between theory and experiments can be resolved with using different experimental techniques such as CS or ESI.

Appendix A. Supplementary data

Supplementary data associated with this article can be found, in the online version, at doi:10.1016/j.ijms.2007.03.002.

References

[1] A.T. Blades, P. Jayaweera, M.G. Ikonomou, P. Kebarle, J. Chem. Phys. 92 (1990) 5900.
[2] A.T. Blades, P. Jayaweera, M.G. Ikonomu, P. Kebarle, Int. J. Mass Spectrom. Ion Proc. 101 (1990) 325.
[3] G. Corongiu, E. Clementi, J. Chem. Phys. 69 (1978) 4885.
[4] G. Akibo-Betts, P.E. Barran, L. Puskar, B. Duncombe, H. Cox, A.J. Stace, J. Am. Chem. Soc. 124 (2002) 9257.
[5] H. Cox, G. Akibo-Betts, R.R. Wright, N.R. Walker, S. Curtis, B. Duncombe, A.J. Stace, J. Am. Chem. Soc. 125 (2003) 233.
[6] C.C. Woodword, M.P. Dobson, A.J. Stace, J. Phys. Chem. 101 (1997) 2279.
[7] R.B. Metz, Int. J. Mass Spectrom. 235 (2) (2004) 131.
[8] D. Schroder, H. Schwarz, J. Phys. Chem. A 103 (37) (1999) 7385.
[9] A.J. Stace, Phys. Chem. Phys. Chem. 3 (11) (2001) 1935.
[10] S.D. Price, Int. J. Mass Spectrom. 260 (2007) 1.
[11] A.J. Stace, N.R. Walker, S. Firth, J. Am. Chem. Soc. 119 (1997) 10239.
[12] A.J. Stace, N.R. Walker, R.R. Wright, S. Firth, Chem. Phys. Lett. 329 (2000) 173.
[13] R.R. Wright, N.R. Walker, S. Firth, A.J. Stace, J. Phys. Chem. A 105 (2001) 54.
[14] A.A. Shvartsburg, K.W.M. Siu, J. Am. Chem. Soc. 123 (2001) 10071.
[15] A.A. Shvartsburg, J.G. Wilkes, J.O. Lay, K.W.M. Siu, Chem. Phys. Lett. 350 (2001) 216.
[16] A.A. Shvartsburg, J. Phys. Chem. A 106 (2002) 4543.
[17] A.A. Shvartsburg, Chem. Phys. Lett. 360 (2002) 479.
[18] A.A. Shvartsburg, J. Am. Chem. Soc. 124 (2002) 12343.
[19] A.A. Shvartsburg, J. Am. Chem. Soc. 124 (2002) 7910.
[20] A.A. Shvartsburg, Chem. Phys. Lett. 376 (2003) 6.
[21] A.A. Shvartsburg, J.B. Wilkes, Int. J. Mass Spectrom. 225 (2003) 155.
[22] C.C. Woodword, M.P. Dobson, A.J. Stace, J. Phys. Chem. 100 (1996) 5605.
[23] M.P. Dobson, A.J. Stace, Chem. Commun. 1533 (1996).
[24] N.R. Walker, S. Firth, A.J. Stace, Chem. Phys. Lett. 292 (1998) 125.
[25] N.R. Walker, R.R. Wright, A.J. Stace, J. Am. Chem. Soc. 121 (2000) 4837.
[26] N.R. Walker, M.P. Dobson, R.R. Wright, P.E. Barran, J.N. Murrell, A.J. Stace, J. Am. Chem. Soc. 122 (2000) 11138.
[27] P.E. Barran, N.R. Walker, A.J. Stace, J. Am. Chem. Soc. 112 (2000) 6173.
[28] N.R. Walker, R.R. Wright, P.E. Barran, J.N. Murrell, A.J. Stace, J. Am. Chem. Soc. 123 (2001) 4223.
[29] A.T. Blades, P. Jayaweera, M.G. Ikonomou, P. Kebarle, Int. J. Mass Spectrom. Ion Process. 102 (1990) 251.
[30] P. Jayaweera, A.T. Blades, M.G. Ikonomou, P. Kebarle, J. Am. Chem. Soc. 112 (1990) 2452.
[31] J.A. Stone, D. Vukomanoic, Chem. Phys. Lett. 346 (2001) 419.
[32] D. Schroeder, H. Schwarz, J. Wu, C. Wesdemiotis, Chem. Phys. Lett. 343 (2001) 258.
[33] S.J. Lippard, J.M. Berg, Principles of Bioinorganic Chemistry, vol. l–24, University Science Books, 1994, p. 194.
[34] D.W. Celander, T.R. Cech, Science 251 (1991) 401.
[35] H.G. Classen, S. Baier, H.F. Schimatschek, C.U. Classen, Magnes. Bull. 17 (3) (1995) 96.
[36] J.E. Sojka, C.M. Weaver, Nutr. Rev. 53 (3) (1995) 71.
[37] D.R. Lide, CRC Handbook of Chemistry and Physics, 84th ed., CRC press, Boca Baton, FL, 2003, p. 10.
[38] A.M. El-Nahas, Chem. Phys. Lett. 365 (2002) 251.
[39] A.M. El-Nahas, N. Tajima, K. Hirao, Chem. Phys. Lett. 318 (2000) 333.
[40] A.M. El-Nahas, Chem. Phys. Lett. Lett. 329 (2000) 176.
[41] A.M. El-Nahas, Chem. Phys. Lett. 345 (2001) 325.
[42] A.M. El-Nahas, Chem. Phys. Lett. 348 (2001) 483.
[43] C. Xiao, K. Walker, F. Hagelberg, A.M. El-Nahas, Int. J. Mass Spectrom. 233 (2004) 87.
[44] T. Shi, K.W.M. Siu, A.C. Hopkinson, Int. J. Mass Spectrom. 255–256 (2006) 251.
[45] H.S.R. Gilson, M. Krauss, J. Phys. Chem. A 102 (1998) 6525.
[46] M.K. Beyer, R.B. Metz, J. Phys. Chem. A 107 (2003) 1760.
[47] J.A. Stone, T. Su, D. Vukomanovic, Can. J. Chem. 83 (2005) 1921.
[48] T. Shi, G. Orlova, J. Guo, D.K. Bohme, A.C. Hopkinson, K.W.M. Siu, J. Am. Chem. Soc. 126 (2004) 7975.
[49] T. Shi, J. Zhao, A.C. Hopkinson, K.W.M. Siu, J. Phys. Chem. B 109 (2005) 10590.
[50] A. Palacios, I. Corral, O. Mó, F. Martín, M. Yáñeza, J. Chem. Phys. 123 (2005) 014315-1.
[51] J. Poater, M. Solá, A. Rimola, L.R. Guez-Santiago, M. Sodupe, J. Phys. Chem. A 108 (2004) 6072.
[52] I. Corral, O. Mó, M. Yáñez, A.P. Scott, L. Radom, J. Phys. Chem. A 107 (2003) 10456.
[53] I. Corral, O. Mó, M. Yáñez, A.P. Scott, L. Radom, J. Phys. Chem. A 109 (2005) 6735.
[54] J.H. Song, J. Kimb, G. Seoa, J.Y. Lee, J. Mol. Struct. (Theochem.) 686 (2004) 147.
[55] M. Beyer, E.R. Williams, V.E. Bondybey, J. Am. Chem. Soc. 121 (1999) 1565.
[56] NIST Chemistry WebBook, see: http://webbook.nist.gov/Chemsitry.
[57] M.J. Frisch, G.W. Trucks, H.B. Schlegel, G.E. Scuseria, M.A. Robb, J.R. Cheeseman, V.G. Zakrzewski, J.A. Montgomery Jr., R.E. Stratmann, J.C. Burant, S. Dapprich, J.M. Millam, A.D. Daniels, K.N. Kudin, M.C. Strain, O. Farkas, J. Tomasi, V. Barone, M. Cossi, R. Cammi, B. Mennucci, C. Pomelli, C. Adamo, S. Clifford, J. Ochterski, G.A. Petersson, P.Y. Ayala, Q. Cui, K. Morokuma, D.K. Malick, A.D. Rabuck, K. Raghavachari, J.B. Foresman, J. Cioslowski, J.V. Ortiz, A.G. Baboul, B.B. Stefanov, G. Liu, A. Liashenko, P. Piskorz, I. Komaromi, R. Gomperts, R.L. Martin, D.J. Fox, T. Keith, M.A. Al-Laham, C.Y. Peng, A. Nanayakkara, C. Gonzalez, M. Challacombe, P.M.W. Gill, B. Johnson, W. Chen, M.W. Wong, J.L. Andres, C. Gonzalez, M. Head-Gordon, E.S. Replogle, J.A. Pople, Gaussian 98W, Revision A.7, Gaussian, Inc., Pittsburgh, PA, 1998.
[58] A.D. Becke, J. Chem. Phys. 98 (1993) 5648.
[59] C. Lee, W. Yang, R.G. Parr, Phys. Rev. B 37 (1988) 785.
[60] P.J. Stephens, F.J. Devlin, C.F. Chabalowski, M.J. Frisch, J. Phys. Chem. 98 (1994) 11623.
[61] G.A. Zhurko, D.A. Zhurko, ChemCraft Version 1.5, 2005.
[62] A.E. Reed, R.B. Weinstock, F.A. Weinhold, J. Chem. Phys. 83 (1985) 735.
[63] J.A. Montgomery Jr., M.J. Frisch, J.W. Ochterski, G.A. Petersson, J. Chem. Phys. 110 (1999) 2822.
[64] J.A. Montgomery Jr., M.J. Frisch, J.W. Ochterski, G.A. Petersson, J. Chem. Phys. 112 (2000) 6532.
[65] E.K. Pokon, M.D. Liptak, S. Feldgus, G.C. Shields, J. Phys. Chem. A 105 (2001) 10483.
[66] C.J. Cramer, Essential of Computational Chemistry: Theories and Methods, Wiley, New York, 2002.
[67] M. Ichihashi, C.A. Corbett, T. Hanmura, J.M. Lisy, T. Kondow, J. Phys. Chem. A 109 (2005) 7872.
[68] T. Ljjima, J. Mol. Struct. 212 (1989) 137.
[69] J. Koput, J. Phys. Chem. A 104 (2000) 10017.
[70] G.S. Hammond, J. Am. Chem. Soc. 77 (1955) 334.
[71] (a) J.P. Butter, D.M.P. Holland, A.C. Parr, R. Stockbauer, Int. J. Mass Spectrom. Ion. Proc. 58 (1984) 1;
(b) P.C. Burgers, J.L. Holmes, Org. Mass Spectrom. 19 (1984) 452.